Eur. Phys. J. A **1**, 307–315 (1998)

THE EUROPEAN PHYSICAL JOURNAL A

Nucleon form factors in a simple three-body quark model ⋆

E. Santopinto[1,2], F. Iachello[1], M.M. Giannini[2]

[1] Center for Theoretical Physics, Sloane Laboratory, Yale University, New Haven, CT 06520-8120, U.S.A
[2] Dipartimento di Fisica dell'Università di Genova, I.N.F.N., Sezione di Genova, via Dodecaneso 33, 16164 Genova, Italy (e-mail:giannini@genova.infn.it)

Received: 15 November 1997
Communicated by V.V. Anisovich

Abstract. We construct a simple 3-body quark model for the non strange nucleon resonances and we give results for the spectrum, the helicity amplitudes and the transition form factors. All the observables, in particular the transition form factors, are evaluated analytically and the results are compared with those of other models.

PACS. 12.39.Jh Nonrelativistic quark model – 13.40.Gp Electromagnetic form factors – 14.20.Gk Baryon resonances with $S = 0$ Protons and neutrons

1 Introduction

Recently there has been a renewed interest in the study of baryon properties [1–8]. Most attention has been devoted to the spectrum and the helicity amplitudes [9–11,1,4–7] but the problem of describing the transition form factors is still open [1–3,12]. On the other hand, the experimental knowledge of the transition form factors is still poor. New accurate and systematic data are expected from the forthcoming experiments at TJNAF (CEBAF).

The non relativistic constituent quark models (CQM) have given good results in the study of the static properties of the nucleon [9,11], like the baryon spectrum and the magnetic moments, and in a qualitative reproduction of the photocouplings [13,14]. The use of harmonic oscillator gives rise to form factors which do not reproduce the experimental data and for this reason it can be interesting to investigate to which extent the results for the transition form factors depend on the choice of the wave functions.

In this article we construct a simple three-body potential model, which gives analytical results for all the observables. In particular, we report on the transition form factors for the electromagnetic excitation of the nucleon.

In Sect. 2 we introduce the hypercentral description of the 3-body problem. In Sect. 3 we construct the model and calculate the spectrum. In Sects. 4 and 5 we calculate the helicity amplitudes and the transitions form factors respectively and compare the results with the experimental data. A brief conclusion is given in Sect. 6.

⋆ Partially supported by EC-contract number ERB FMRX-CT96-0008

2 The three-body problem

We consider non-strange baryons as a bound state of three constituent quarks. After removal of the center of mass coordinate, $\boldsymbol{R}$, the configurations of three particles are described by the Jacobi coordinates, $\boldsymbol{\rho}$ and $\boldsymbol{\lambda}$,

$$\boldsymbol{\rho} = \frac{1}{\sqrt{2}}(\boldsymbol{r}_1 - \boldsymbol{r}_2),$$
$$\boldsymbol{\lambda} = \frac{1}{\sqrt{6}}(\boldsymbol{r}_1 + \boldsymbol{r}_2 - 2\boldsymbol{r}_3). \quad (1)$$

Instead of $\boldsymbol{\rho}$ and $\boldsymbol{\lambda}$, one can introduce the hyperspherical coordinates, which are given by the angles $\Omega_\rho = (\theta_\rho, \phi_\rho)$ and $\Omega_\lambda = (\theta_\lambda, \phi_\lambda)$ together with the hyperradius, x, and the hyperangle, ξ, defined respectively by [15,16]

$$x = \sqrt{\boldsymbol{\rho}^2 + \boldsymbol{\lambda}^2}, \quad \xi = arctg(\frac{\rho}{\lambda}). \quad (2)$$

As a model of light baryons, we consider three identical quarks of mass m with Hamiltonian

$$H = \frac{\boldsymbol{p}_\rho^2}{2m} + \frac{\boldsymbol{p}_\lambda^2}{2m} + V(x), \quad (3)$$

where the potential $V(x)$ is assumed to depend on x only, that is to be hypercentral. Since $x = (\boldsymbol{\rho}^2 + \boldsymbol{\lambda}^2)^{\frac{1}{2}}$, the interaction in (3) is not purely a two-body interaction, but it contains three-body terms.

Several authors [17–20,4,21] have suggested that three-body interactions can play an important role in hadrons, since the non-abelian nature of QCD leads to gluon-gluon couplings which, in turn, can produce three-body forces. It is also interesting to notice that two-body interactions can

be well approximated by a hypercentral potential [22–25], specially for the lower part of the spectrum.

Using hyperspherical coordinates, the kinetic energy operator of a three-body problem can be written as:

$$-\frac{1}{2m}(\Delta_\rho + \Delta_\lambda) = -\frac{1}{2m}(\frac{\partial^2}{\partial x^2} + \frac{5}{x}\frac{\partial}{\partial x} - \frac{L^2(\Omega_\rho, \Omega_\lambda, \xi)}{x^2}), \tag{4}$$

where $L^2(\Omega_\rho, \Omega_\lambda, \xi)$ is the quadratic Casimir operator of the six dimensional rotation group, $O(6)$, and its eigenfunctions are the hyperspherical harmonics $Y_{[\gamma]l_\rho l_\lambda}(\Omega_\rho, \Omega_\lambda, \xi)$

$$L^2(\Omega_\rho, \Omega_\lambda, \xi)Y_{[\gamma]l_\rho l_\lambda}(\Omega_\rho, \Omega_\lambda, \xi) = \gamma(\gamma+4)Y_{[\gamma]l_\rho l_\lambda}(\Omega_\rho, \Omega_\lambda, \xi), \tag{5}$$

with the grand-angular quantum number, γ, given by $\gamma = 2v + l_\rho + l_\lambda$, and $v = 0, 1, ...$ and l_ρ and l_λ being the angular momenta associated with the $\boldsymbol{\rho}$ and $\boldsymbol{\lambda}$ variables. The hyperspherical harmonics are written as products of standard spherical harmonics, trigonometric functions and Jacobi polynomials (see [16]).

If there is hyperrotational $O(6)$ invariance (i.e. if the quark potential is hypercentral, depending on the hyperradius x only), each eigenfunction can be factorized into a hyperradial part, $\psi_\gamma(x)$, and a hyperangular part, $Y_{[\gamma]l_\rho l_\lambda}(\Omega)$. The hyperradial wave function $\psi_\gamma(x)$ is a solution of the equation

$$[\frac{d^2}{dx^2} + \frac{5}{x}\frac{d}{dx} - \frac{\gamma(\gamma+4)}{x^2}]\psi_\gamma(x) = -2m[E - V(x)]\psi_\gamma(x). \tag{6}$$

This equation can be solved analytically in two cases [22, 20]:

$$V(x)_{h.o.} = \frac{3}{2}kx^2 \tag{7}$$

(six-dimensional harmonic oscillator) and

$$V_{hyc}(x) = -\frac{\tau}{x} \tag{8}$$

(six-dimensional Coulomb problem). We can observe that the two-body harmonic oscillator potential $\sum_{i<j}\frac{1}{2}kr_{ij}^2 = \frac{3}{2}kx^2$ that means that it can be written as a hypercentral potential. The h.o. is used as a basis in the approach of [9].

The use of a hyperCoulomb interaction in baryon structure was suggested long ago [26] following earlier observations that the low-lying spectrum of hadrons has a hydrogenlike structure [27]. In the case of the potential of (8), all results for the three-quark problem can be obtained in closed analytic form, thus providing an alternative basis to the harmonic oscillator.

The solution of the hyperCoulomb problem can be simply obtained by generalizing to six dimensions the calculations for the usual Coulomb problem in three dimensions, obtaining

$$E_{n,\gamma} = -\frac{\tau^2 m}{2n^2}, \tag{9}$$

where $n = \gamma + \frac{5}{2} + n'$ is the principal quantum number and $n' = 0, 1, 2, ...$ is the radial quantum number that counts the number of nodes of the wave function. The hyperCoulomb potential has a symmetry $O(7)$, larger than the $O(6)$-symmetry which is shared with every hypercentral potential. The dynamic symmetry $O(7)$ of the hyperCoulomb problem can be used to obtain the eigenvalues using purely algebraic methods. In fact, the hyperCoulomb Hamiltonian can be rewritten as [21]

$$H = -\frac{\tau^2 m}{2[C_2(O(7)) + \frac{25}{4}]}, \tag{10}$$

where $C_2(O(7))$ is the quadratic Casimir invariant of $O(7)$. By observing that the eigenvalues of $C_2(O(7))$ in the totally symmetric representations of $O(7)$, $(\omega, 0, 0)$, are $\omega(\omega+5)$ [28], one obtains directly the eigenvalues

$$E = -\frac{\tau^2 m}{2[\omega(\omega+5) + 25/4]},\ \omega = 0, 1, ...\infty. \tag{11}$$

The quantum number ω is related to n and γ by $n = \omega + \frac{5}{2}$, where $\omega = \gamma + n'$.

The eigenfunctions of (6) with the hyperCoulomb potential can be obtained analytically and are

$$\psi_{\omega\gamma}(x) = \left[\frac{(\omega-\gamma)!(2g)^6}{(2\omega+5)(\omega+\gamma+4)!^3}\right]^{\frac{1}{2}} \times (2gx)^\gamma e^{-gx} L_{\omega-\gamma}^{2\gamma+4}(2gx), \tag{12}$$

where for the associated Laguerre polynomials we have used the notation of [29] and $g = \frac{\tau m}{\omega+\frac{5}{2}}$.

The hyperradial wave functions, $\psi_{\omega\gamma}(x)$, depending on x, are totally symmetric for exchange of the quark coordinates. They must be completed with the appropriate combinations of hyperspherical harmonics which not only have definite total angular momentum L but also transform according to an irreducible representation of the permutation group of three identical objects, S_3. The problem of finding combinations of hyperspherical harmonics with definite transformation properties for S_3 has been solved in different ways [30,31,21]. In Table 1 we report the results.

The complete wave functions contain a hyperradial, hyperangular, spin, flavor and color part. The orbital angular momentum L and spin S of the three quarks are coupled to the total angular momentum J. The colour part is completely antisymmetric and the hyperradial part, which depends only on x, is completely symmetric. Therefore, the remaining part must be completely symmetric. In practice, this means that the complete wave functions are those of [9], written in terms of hyperspherical coordinates, x, ξ, Ω_ρ, Ω_λ, where the harmonic oscillator part is substituted by the hyperCoulomb function $\psi_{\omega\gamma}(x)$ of (12). The complete baryon states are reported in Appendix A.

An interesting property of the spectrum of the hyperCoulomb potential is the degeneracy of the first excited $L = 0$ state and the $L = 1$ states, both belonging to the representation $(1, 0, 0)$ of $O(7)$ (see Fig. 1).

Table 1. Combinations $(Y_{[\gamma]l_\rho l_\lambda})_{S_3}$ of the hyperspherical harmonics $Y_{[\gamma]l_\rho l_\lambda}$ that transform as irreducible representations of S_3. For simplicity of notation, in the third column we have omitted the coupling of l_ρ and l_λ to the total angular momentum L given in the second column

γ	$L^P_{S_3}$	$(Y_{[\gamma]l_\rho l_\lambda})_{S_3}$	S_3
0	0^+_S	$Y_{[0]00}$	S
1	1^-_M	$Y_{[1]10}$	M_ρ
		$Y_{[1]01}$	M_λ
2	2^+_S	$\frac{1}{\sqrt{2}}[Y_{[2]20}+Y_{[2]02}]$	S
	2^+_M	$Y_{[2]11}$	M_ρ
		$\frac{1}{\sqrt{2}}[Y_{[2]20}-Y_{[2]02}]$	M_λ
	1^+_A	$Y_{[2]11}$	A
	0^+_M	$Y_{[2]11}$	M_ρ
		$Y_{[2]00}$	M_λ

The near degeneracy of the states with $L=0$ [$N(1440)P_{11}$] and $L=1$ [$N(1520)D_{13}$, $N(1535)S_{11}$,...] is a characteristic of the experimental spectrum of the nucleon. This feature cannot be reproduced in models with only two-body forces since the excited $L=0$ state, having one more node, must always lie above the $L=1$ state, as shown in [32].

However, the hyperCoulomb potential produces a spectrum which converges to zero for large values of ω. In order to provide a realistic description of the spectrum, one must add a confining interaction to the hyperCoulomb term.

3 The spectrum

The hyperCoulomb potential does not confine quarks in hadrons and therefore one has to add a confining term. From lattice calculations and other considerations [33, 18] one expects to have a linear potential. The potential we use is

$$V(x) = -\frac{\tau}{x} + \beta x. \tag{13}$$

The solution of the hypercentral (6) with this potential cannot be obtained analytically, except when the linear term is treated as a perturbation. We consider here this situation, which is valid, to a good approximation, for the low-lying states.

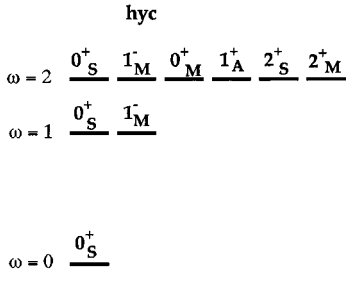

Fig. 1. Schematic representation of the low-lying spectrum of the hyperCoulomb potential. The total orbital angular momentum, the parity and the S_3-symmetry (S,A,M) are reported on top of each levels

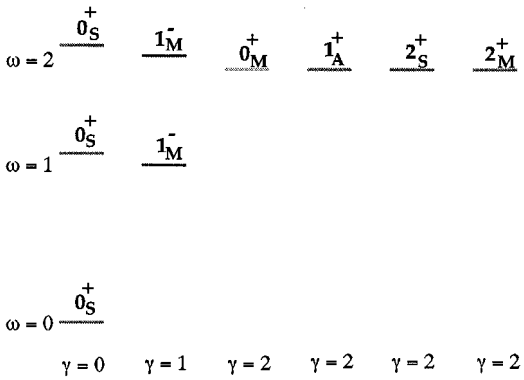

Fig. 2. Schematic representation of the low-lying spectrum of the hyperCoulomb potential with linear confinement. The total orbital angular momentum, the parity and the S_3-symmetry (S,A,M) are reported on top of each level. On the bottom the grand-angular quantum number γ is reported

The energy eigenvalues can be obtained analytically and are given by

$$E_{n,\gamma} = -\frac{\tau^2 m}{2n^2} + \frac{\beta}{2m\tau}[3n^2 - \gamma(\gamma+4) - \frac{15}{4}], \tag{14}$$

The confining term removes the $O(7)$ degeneracy and leaves only an $O(6)$ degeneracy (see Fig. 2).

On the basis of some general arguments (for example one-gluon exchange contributions) one expects additional quark-quark interactions which are spin dependent, in particular a spin-spin interaction, a spin-orbit interaction and a tensor one. We do not consider spin-orbit forces, for which there is little evidence in hadrons, and we make the following model for the spin-spin and tensor interactions

$$V^S(x) = Ae^{-\alpha x}\sum_{i<j}\boldsymbol{\sigma}_i\cdot\boldsymbol{\sigma}_j = \tag{15}$$

$$= Ae^{-\alpha x}[2S^2 - \frac{9}{4}], \tag{16}$$

where S is the total spin of the 3-quark system,

$$V^T(x) = B\frac{1}{x^3}\sum_{i<j}\left[\frac{(\boldsymbol{\sigma}_i\cdot(\boldsymbol{r}_i-\boldsymbol{r}_j))\,(\boldsymbol{\sigma}_j\cdot(\boldsymbol{r}_i-\boldsymbol{r}_j))}{|\boldsymbol{r}_i-\boldsymbol{r}_j|^2} - \frac{1}{3}(\boldsymbol{\sigma}_i\cdot\boldsymbol{\sigma}_j)\right]. \tag{17}$$

We note that for one-gluon exchange, the coordinate dependence of V^S is $\delta(\boldsymbol{r}_{ij})$ [9], while in algebraic approaches [1] this dependence is taken to be a constant.

Using the states of Appendix A, the matrix elements of the spin-dependent interactions (16, 17) can be evaluated analytically. The diagonalization is performed numerically and the results depend on the strength A, the ratio $\frac{\alpha}{\tau}$ and B. Contrary to the case of one gluon exchange, the spin-spin interaction of (16) acts on all states, while for a delta function dependence only $L=0$ states are affected. With

Table 2. Comparison between the calculated masses of non-strange baryon resonances below 2 GeV, M_{calc}, and the experimental masses [33], M_{exp}

Baryon	Status	M_{exp} (MeV)	J^π	$\omega\ \gamma\ L^\pi$	S	S_3	M_{calc} (MeV)
N(938) P_{11}	****	938	$\frac{1}{2}^+$	$0\ 0\ 0^+$	$\frac{1}{2}$	S	938
$\Delta(1232)P_{33}$	****	1232	$\frac{3}{2}^+$	$0\ 0\ 0^+$	$\frac{3}{2}$	S	1237
N(1440) P_{11}	****	1440	$\frac{1}{2}^+$	$1\ 0\ 0^+$	$\frac{1}{2}$	S	1562
$\Delta(1600)P_{33}$	***	1600	$\frac{3}{2}^+$	$1\ 0\ 0^+$	$\frac{1}{2}$	S	1675
N(1535) S_{11}	****	1535	$\frac{1}{2}^-$	$1\ 1\ 1^-$	$\frac{1}{2}$	M	1543
N(1520) D_{13}	****	1520	$\frac{3}{2}^-$	$1\ 1\ 1^-$	$\frac{1}{2}$	M	1544
N(1650) S_{11}	****	1650	$\frac{1}{2}^-$	$1\ 1\ 1^-$	$\frac{3}{2}$	M	1665
N(1700) D_{13}	***	1700	$\frac{3}{2}^-$	$1\ 1\ 1^-$	$\frac{3}{2}$	M	1679
N(1675) D_{15}	****	1675	$\frac{5}{2}^-$	$1\ 1\ 1^-$	$\frac{3}{2}$	M	1671
$\Delta(1620)S_{31}$	****	1620	$\frac{1}{2}^-$	$1\ 1\ 1^-$	$\frac{1}{2}$	M	1544
$\Delta(1700)D_{33}$	****	1700	$\frac{3}{2}^-$	$1\ 1\ 1^-$	$\frac{1}{2}$	M	1544
N(1710) P_{11}	***	1710	$\frac{1}{2}^+$	$2\ 0\ 0^+$	$\frac{1}{2}$	M	1819
N(1720) P_{13}	****	1720	$\frac{3}{2}^+$	$2\ 2\ 2^+$	$\frac{1}{2}$	S	1819
N(1680) F_{15}	****	1680	$\frac{5}{2}^+$	$2\ 2\ 2^+$	$\frac{1}{2}$	S	1819
$\Delta(1910)P_{31}$	****	1910	$\frac{1}{2}^+$	$2\ 2\ 2^+$	$\frac{3}{2}$	S	1863
$\Delta(1920)P_{33}$	***	1920	$\frac{3}{2}^+$	$2\ 2\ 2^+$	$\frac{3}{2}$	S	1819
$\Delta(1905)F_{35}$	****	1905	$\frac{5}{2}^+$	$2\ 2\ 2^+$	$\frac{3}{2}$	S	1819
$\Delta(1950)F_{37}$	****	1950	$\frac{7}{2}^+$	$2\ 2\ 2^+$	$\frac{3}{2}$	S	1864
$\Delta(1900)S_{31}$	***	1900	$\frac{1}{2}^-$	$2\ 1\ 1^-$	$\frac{1}{2}$	M	1829

hydrogenic wave functions, the effect of the tensor interaction is rather small, contrary to the case of harmonic oscillator wave functions.

We can now compare the results of this model with the experimental spectrum. In absence of spin-spin interactions, masses are given by (14), to which a constant should be added

$$M = E_0 - \frac{\tau^2 m}{2n^2} + \frac{\beta}{2m\tau}[3n^2 - \gamma(\gamma+4) - \frac{15}{4}], \qquad (18)$$

in order that for $n = \frac{5}{2}$ and $\gamma = 0$ the nucleon mass is reproduced. There are two strength parameters here: τ and β from the hyperCoulomb and the confining term. These parameters can be fitted to the observed resonance masses, with values $\tau = 6.39$, and $\beta = 0.148 fm^{-2}$, considering a quark mass about one third of the nucleon mass. In finding the values of the parameters in absence of spin-spin interactions, an average is taken over different states with the same quantum numbers ω, γ and different spin ($\frac{1}{2}$ or $\frac{3}{2}$).

The spin-spin interaction depends on two parameters, A and α. These two parameters are determined from the $N(939) - \Delta(1232)$ and the $N(1535) - N(1650)$ splittings. The resulting values are $A = 140.7 MeV$ and $\alpha = 1.53 fm^{-1}$, a relatively long range. This means that with hydrogenic wave functions, which are not so concentrated near the origin as the harmonic oscillator ones, a spin-spin interaction with non-zero range is necessary in order to reproduce the observed splittings. On the other hand, the origin of the spin-spin dependent interaction can be ascribed not only to the zero-range one-gluon exchange interaction, but also to more complicated exchange mechanisms.

The tensor interaction depends on the parameter B. Since with hydrogenic wave functions the effects of the tensor interaction is very small, we have no way to determine this parameter. However, with values of B of the order of $\approx 14 MeV fm^3$, the description of the spectrum is slightly improved, although the overall effect of the tensor interaction is small. Our final results, summarized in Table 2, show that this model provides a reasonable description of the observed resonances, specially for the lower part of the spectrum because of the approximation used for the confining term.

4 The helicity amplitudes

The reproduction of the spectrum is not a sufficient test for a model. A further test is provided by the analysis of the electromagnetic properties, as the helicity amplitudes and the transition form factors. The helicity amplitudes describe the photoexcitation of the nucleon to a baryon resonance. Up to now they have been extracted from pion-photoproduction and their present knowledge is affected by a certain amount of model dependence, mainly due to some ingredients (resonance propagators, strong decay vertices,..) which are necessary in order to analyze experimental data. Nevertheless they are the necessary input for the theoretical calculation of a variety of fundamental processes, like photoproduction of mesons (π, η, K,...) and Compton scattering.

The helicity amplitudes are defined as

$$A_{3/2} = \langle B, J_z = \tfrac{3}{2} \, |H_{em}|N, J_z = \tfrac{1}{2} \, \rangle$$
$$A_{1/2} = \langle B, J_z = \tfrac{1}{2} \, |H_{em}|N, J_z = -\tfrac{1}{2} \, \rangle, \quad (19)$$

where B denotes a resonance (N* or Δ) and H_{em} is the transverse electromagnetic interaction. The electromagnetic interaction is given by a direct photon-quark coupling and is written in the non-relativistic approximation as [13,14]

$$H_{em} = -\sum_{j=1}^{3} \left[\frac{e_j}{2m_j} (\boldsymbol{p}_j \cdot \boldsymbol{A}_j + \boldsymbol{A}_j \cdot \boldsymbol{p}_j) + 2\mu_j \boldsymbol{s}_j \cdot (\nabla \times \boldsymbol{A}_j) \right], \quad (20)$$

where $e_j, m_j, \boldsymbol{s}_j, \boldsymbol{p}_j$ and $\mu_j = \frac{e_j}{2m_j}$ denote, respectively, the electric charge, the mass, the spin, the momentum and the magnetic moment of the j-th quark and $\boldsymbol{A}_j = \boldsymbol{A}_j(\boldsymbol{r}_j)$ is the photon field.

The baryon states have been determined in the previous sections and are given in Appendix A. All the parameters of the model have been fixed on the baryon spectrum and the $SU(6)$-mixing due to the spin-dependent interactions of Section 3 is taken into account for all baryon states. We evaluate the amplitudes in the equal momentum frame or Breit frame,

$$k^2 = Q^2 + \frac{(W^2 - M^2)^2}{2(W^2 + M^2) + Q^2}, \quad (21)$$

where M is the nucleon mass, W is the mass of the resonance, and $Q^2 = \boldsymbol{k}^2 - {k_0}^2$ is the mass squared of the photon with tetramomentum $(k_0, \boldsymbol{k})$.

In Tables 3 and 4 we report the calculated helicity amplitudes for the proton and the neutron compared with the compilation of the PDG [34]. One can see the effect of including the spin dependent interaction, particularly important for those resonances, as the $S_{11}(1650)$ etc., which, without a $SU(6)$-breaking term, would be identically zero. One can see that our results are quite similar to the h.o. ones and so one can conclude that the calculated helicity amplitudes depend on what the two models have in common, that is the $SU(6)$ (spin-flavour) structure of the states. Since the spectrum and the helicity amplitudes do not allow to discriminate among the various models, is important to study other observables, like the form factors, which depend strongly on details of the wave functions.

5 Form factors

All electromagnetic form factors (transverse, longitudinal and scalar) of interest can be expressed in terms of two elementary spatial matrix elements [1]

$$F(k) = \langle f|U|i\rangle, \; G_\mu(k) = \langle f|T_\mu|i\rangle, \quad (22)$$

Table 3. The helicity amplitudes for the nucleon resonances calculated in our model with and without spin-dependent interactions reported in column I and II respectively, in comparison with the results of [32] (column KI) and the experimental data from the PDG [33]. We consider only the resonances with a 4− or 3−star classification, for both their status and photocouplings. Units are 10^{-3} $(GeV)^{-\frac{1}{2}}$

Baryon		Exp	I	II	KI
N(1440) P_{11}	p 1/2	-72 ± 9	-64	-53	-24
	n 1/2	52 ± 25	43	36	16
N(1520) D_{13}	p 1/2	-22 ± 8	-44	-41	-23
	n 1/2	-62 ± 6	-12	-15	-45
	p 3/2	163 ± 7	68	74	128
	n 3/2	-137 ± 13	-67	-74	-122
N(1535) S_{11}	p 1/2	68 ± 10	114	120	147
	n 1/2	-59 ± 22	-77	-80	-119
N(1650) S_{11}	p 1/2	52 ± 17	10	0	88
	n 1/2	-11 ± 28	16	21	-35
N(1675) D_{15}	p 1/2	18 ± 10	0	0	12
	n 1/2	-50 ± 14	-30	-28	-37
	p 3/2	18 ± 9	0	0	16
	n 3/2	-70 ± 6	-43	-40	-53
N(1680) F_{15}	p 1/2	-14 ± 8	-19	-17	0
	n 1/2	27 ± 10	20	19	26
	p 3/2	135 ± 17	17	17	91
	n 3/2	35 ± 11	-1	0	-25
N(1710) P_{11}	p 1/2	-6 ± 27	20	19	-47
	n 1/2	16 ± 29	-7	-6	-21

Table 4. The same as in Table 3 for the Δ resonances

Baryon		Exp	I	II	KI
$\Delta(1232)P_{33}$	N 1/2	-141 ± 5	-106	-107	-103
	N 3/2	-257 ± 8	-183	-185	-179
$\Delta(1620)S_{31}$	N 1/2	30 ± 14	41	41	59
$\Delta(1700)D_{33}$	N 1/2	114 ± 13	74	71	100
	N 3/2	91 ± 29	76	74	105
$\Delta(1905)F_{35}$	N 1/2	-37 ± 16	-7	-5	8
	N 3/2	-31 ± 30	-24	-22	-33
$\Delta(1950)F_{37}$	N 1/2	-85 ± 17	-13	-13	-50
	N 3/2	-101 ± 14	-17	-16	-69

where i and f represent initial and final states and

$$U = e^{-ik\sqrt{\frac{2}{3}}\lambda_z}, T_\mu = imk_0\sqrt{\frac{2}{3}}\lambda_\mu e^{-ik\sqrt{\frac{2}{3}}\lambda_z}, \mu = 0, \pm 1. \quad (23)$$

In (23), $(k_0, \boldsymbol{k})$ is the virtual photon tetra-momentum, with $\boldsymbol{k} = \boldsymbol{p}_f - \boldsymbol{p}_i$ taken to be in the z-direction. The T_μ operator is the operator written in (20) after replacing $\frac{\boldsymbol{p}}{m}$ with $ik_0\boldsymbol{r}$ [35]. The form factors $F(k)$ and $G_\mu(k)$ can all be evaluated in explicit analytic form in this model. The matrix elements of the operator U of (23) to be evaluated are of the type

$$\int d^3\rho d^3\lambda \psi_{\omega'\gamma'}(x) Y_{[\gamma']}(\xi, \Omega_\rho, \Omega_\lambda) \times e^{-i\eta k\lambda_z} \psi_{\omega\gamma}(x) Y_{[\gamma]}(\xi, \Omega_\rho, \Omega_\lambda), \quad (24)$$

where $\eta = \sqrt{\frac{2}{3}}$ and the initial state is the ground state given by

$$\psi_{\omega\gamma}(x)Y_{[\gamma]}(\xi,\Omega_\rho,\Omega_\lambda) = [\frac{(2g_0)^6}{5(4!)}]^{1/2} e^{-g_0 x} \frac{1}{\sqrt{4\pi}} \frac{1}{\sqrt{4\pi}} \frac{4}{\sqrt{\pi}}, \tag{25}$$

with $\omega = 0$, $\gamma = 0$ and $g_0 = \frac{2}{5}\tau m$.

The integrals of interest can be evaluated in terms of two basic integrals:
(a) The integral representation of the ordinary Bessel functions

$$\int_0^\pi d\xi sin^{2\beta}\xi e^{iz\cos\xi} = \sqrt{\pi}\Gamma(\beta+\frac{1}{2})2^\beta \frac{J_\beta(z)}{z^\beta}, \tag{26}$$

from which one can derive, by taking derivatives with respect to z, the related formula

$$\int_0^\pi d\xi sin^{2\beta}\xi cos^\alpha\xi e^{iz\cos\xi} = \sqrt{\pi}\Gamma(\beta+\frac{1}{2})2^\beta \frac{d^\alpha}{dz^\alpha}[\frac{J_\beta(z)}{z^\beta}](-i)^\alpha. \tag{27}$$

Straightforward manipulations of these formulas lead, for example, to

$$\int_0^{\pi/2} d\xi \sin^2\xi\cos^2\xi j_0(z\cos\xi) = \frac{\pi}{2}\frac{J_2(z)}{z^2}. \tag{28}$$

To obtain integrals involving $j_l(z\cos\xi)$, one uses the recurrence relations of the spherical Bessel functions

$$j_l(z) = z^l(-\frac{1}{z}\frac{d}{dz})^l j_0(z). \tag{29}$$

(b) The Laplace transform of the ordinary Bessel functions

$$\int_0^\infty dx x^\beta J_\beta(ax)e^{-sx} = \frac{\Gamma(\beta+\frac{1}{2})}{\sqrt{\pi}}\frac{(2a)^\beta}{(s^2+a^2)^{\beta+\frac{1}{2}}}, \tag{30}$$

from which one can obtain, by taking derivatives,

$$\int_0^\infty dx x^{\beta+h} J_\beta(ax)e^{-sx} = \frac{\Gamma(\beta+\frac{1}{2})}{\sqrt{\pi}}(2a)^\beta(-1)^h\frac{d^h}{ds^h}\frac{1}{(s^2+a^2)^{\beta+\frac{1}{2}}}. \tag{31}$$

Using these formulas we have, for example,

$$\int_0^\infty dx x^3 J_2(\eta k x)e^{-sx} = \frac{3}{4}(2\eta k)^2\frac{5}{2}\frac{2s}{(s^2+\eta^2k^2)^{\frac{7}{2}}}, \tag{32}$$

For example using (28) and (32), one obtains the elastic form factor

$$F_0(k) = \frac{1}{[1+(\frac{\eta k}{2g_0})^2]^{\frac{7}{2}}}. \tag{33}$$

All other form factors can be obtained in a similar way and the analytical results are reported in Table 5.

In addition to the form factors $F(k)$, one also needs the form factors $G_\mu(k)$ of (22), (23). These form factors, however, can be obtained from the previous ones, $F(k)$, by noting that the matrix elements of the operator T_z ($\mu = 0$) are related to those of U by

$$\langle f|T_z|i\rangle = \frac{\eta'}{i\eta}\frac{\partial}{\partial k}\langle f|U|i\rangle \tag{34}$$

where $\eta' = imk_0\eta$.

Table 5. The scalar form factors $F(k)$ of (22) for transitions to final states labelled by ω, γ, $L^P_{S_3}$. The initial state is $0,0,0^+_S$ and $a = \frac{\eta}{2g_0}$

ω	γ	$L^P_{S_3}$	$\langle\omega\gamma L^P_{S_3}\|U\|000^+_S\rangle$
0	0	0^+_S	$\frac{1}{(1+k^2a^2)^{7/2}}$
1	1	1^-_M	$-i\sqrt{7}(\frac{5}{6})^4(\frac{7}{6})^4\frac{ka}{(1+\frac{49}{36}k^2a^2)^{9/2}}$
1	0	0^+_S	$\sqrt{7}(\frac{7}{6})^5(\frac{5}{6})^4\frac{(ka)^2}{(1+\frac{49}{36}k^2a^2)^{9/2}}$
2	2	2^+_S	$-\frac{\sqrt{21}}{\sqrt{2}}(\frac{5}{7})^5(\frac{9}{7})^5\frac{(ka)^2}{(1+\frac{81}{49}k^2a^2)^{11/2}}$
2	2	2^+_M	$\frac{\sqrt{21}}{\sqrt{2}}(\frac{5}{7})^5(\frac{9}{7})^5\frac{(ka)^2}{(1+\frac{81}{49}k^2a^2)^{11/2}}$
2	2	0^+_M	$-\frac{1}{2}\sqrt{21}(\frac{5}{7})^5(\frac{9}{7})^3\frac{\frac{81}{49}(ka)^2}{(1+\frac{81}{49}k^2a^2)^{11/2}}$
2	1	1^-_M	$-i\frac{\sqrt{7}}{3}(\frac{5}{7})^4(\frac{9}{7})^5\frac{(ka)[1+\frac{486}{49}(ka)^2]}{(1+\frac{81}{49}k^2a^2)^{11/2}}$
2	0	0^+_S	$\frac{\sqrt{3}}{2}(\frac{5}{7})^4(\frac{9}{7})^5\frac{(ka)^2[1+\frac{486}{49}(ka)^2]}{(1+\frac{81}{49}k^2a^2)^{11/2}}$

It is interesting to compare the form factors of Table 5 with those of the harmonic oscillator quark model. For small k, both models have obviously the same behavior. For very large k the non relativistic approximation is not applicable but it is interesting to note that already for intermediate values of k the two models exhibit different behaviors. The h.o. form factors decrease as gaussians, while the hyperCoulomb ones decrease as powers of k, although the powers are not really coincident with the observed ones. For example, the experimental elastic form factor G^p_E decreases as

$$G^p_E(k) = \frac{1}{(1+k^2a^2)^2}, \tag{35}$$

to be compared with (33) Another important property of the form factors $F(k)$, which is absent in the h.o. case, is that the transition radius increases drastically with ω. Already for $\omega = 1$, the transition radius is $\frac{7}{6}a$, i.e. 17% larger than the radius a of the ground state $\omega = 0$. The drastic increase in the radii of the nucleon resonances is at the basis of their Regge behavior, with linearly rising trajectories, although the increase provided by this model is somewhat smaller than what is needed to reproduce the experimental data.

The transverse helicity amplitudes $A_{1/2}$, $A_{3/2}$, which are combinations of the form factors $F(k)$ and $G_\mu(k)$, as functions of the momentum transfer, are reported in Figs. 3,4 and 5 and compared with the experimental data and the h.o. results. We limit ourselves to the transition to the low-lying resonances since, because of the approximations we have made, they are better reproduced.

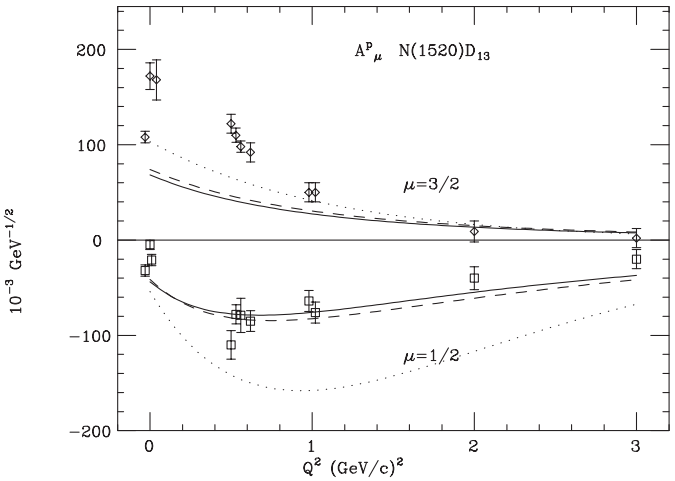

Fig. 3. The helicity amplitudes $A^p_{3/2}$,$A^p_{1/2}$, in the Breit frame for the excitation of the $D13(1520)$ resonance. The *full curve* is the complete result of our model, while the *dashed curve* is the result without spin-dependent interactions. The experimental data are taken from [35]

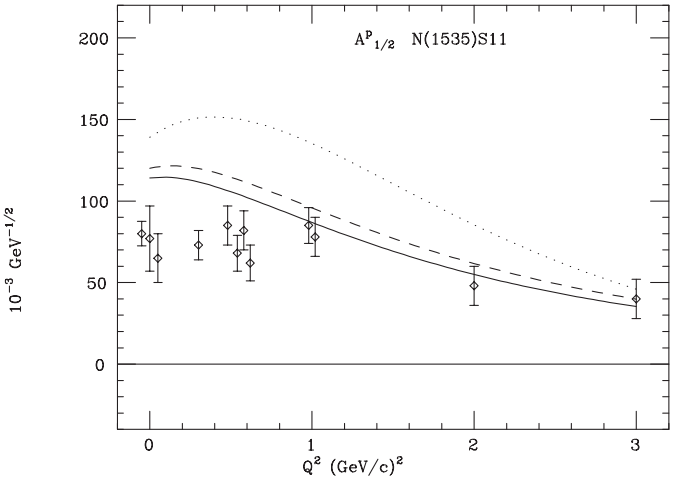

Fig. 4. The same as in Fig. 3 for the excitation of the $S11(1535)$ resonance

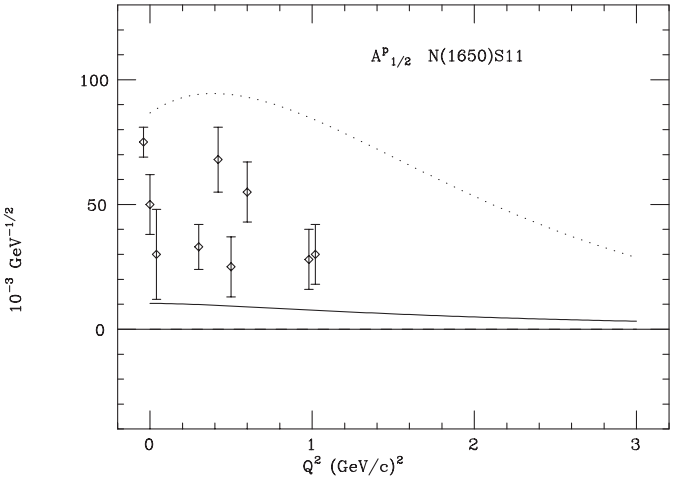

Fig. 5. The same as in Fig. 3 for the excitation of the $S11(1650)$ resonance

We present the results with and without the spin-dependent interactions (16, 17). In general the effect of the $SU(6)$-breaking on the helicity form factors is small apart from some few cases, such as the $S11(1650)$, where in absence of spin dependent interactions the transition amplitude for the proton would be identically zero.

In Fig. 3 we report the results for the proton helicity amplitudes of the $D_{13}(1520)$-resonance. The curves with and without the spin-spin interactions are quite the same. The behaviour at medium momentum transfer is quite well reproduced, while at low Q^2 there are problems, specially for the strength of the $A_{3/2}$-amplitude. Also the h.o. curves obtained with the value of the α-parameter ($\alpha = 0.41GeV$, corresponding to a confinement radius of the order of $0.5fm$) which reproduces the helicity amplitudes and in particular the $A_{3/2}$-amplitude for $D_{13}(1520)$-resonance [13,14], exhibit a lack of strength at low Q^2, while the Q^2-behaviour of $A_{1/2}$ is far from the data.

In Fig. 4 we report the results for the proton helicity amplitudes of the $S_{11}(1535)$-resonance, and the conclusions are similar as for Fig. 3, in particular again there are problems with the behaviour at low Q^2.

In Fig. 5 we give the results for the $S_{11}(1650)$-resonance. For this resonance the spin-spin mixing is determinant since otherwise the transition amplitude would be zero.

The results reported in Figs. 3, 4 and 5 show clearly that the transition form factors depend strongly on the quark wave functions and so they can provide a sensitive test of quark dynamics.

6 Discussion and conclusions

In this article we have studied a simple three-body model of non-strange baryons. The model reproduces, although not exactly, three of the features of the baryon phenomenology: the power-law behaviour of the form factors, the near degeneracy of 1^-_M and 0^+_S states and the increase in transition radii with increasing excitation energy. It has also drawbacks which come from the approximations we have done. In particular one should reproduce better the higher part of the spectrum, the low Q^2-behaviour of the transition form factors and take into account relativistic corrections, for example following the lines of [10]. In any case, this simple model can be considered as a starting point for more refined investigations.

This work was supported in part by D.O.E., Contract DE-FG02-91-ER 40608, and in part by I.N.F.N.

Appendix A

In Tables 6 and 7, we give the explicit form of the three-quark states with both positive and negative parity of in-

Table 6. Three-quark states with positive parity. For simplicity of notation, we have omitted the coupling to the total angular momentum L of the second column

Resonance	$L^P_{S_3}$	S	T	SU(6) configurations
$P11$	0^+_S	$\frac{1}{2}$	$\frac{1}{2}$	$\psi_{00}Y_{[0]00}\Omega_S$
	0^+_S	$\frac{1}{2}$	$\frac{1}{2}$	$\psi_{10}Y_{[0]00}\Omega_S$
	0^+_S	$\frac{1}{2}$	$\frac{1}{2}$	$\psi_{20}Y_{[0]00}\Omega_S$
	0^+_M	$\frac{1}{2}$	$\frac{1}{2}$	$\psi_{22}\frac{1}{\sqrt{2}}[Y_{[2]00}\Omega_{MS}+Y_{[2]11}\Omega_{MA}]$
	2^+_M	$\frac{3}{2}$	$\frac{1}{2}$	$\psi_{22}\frac{1}{\sqrt{2}}[\frac{1}{\sqrt{2}}(Y_{[2]20}-Y_{[2]02})\phi_{MS}+Y_{[2]11}\phi_{MA}]\chi_S$
$P13$	2^+_M	$\frac{1}{2}$	$\frac{1}{2}$	$\psi_{22}\frac{1}{\sqrt{2}}[\frac{1}{\sqrt{2}}(Y_{[2]20}-Y_{[2]02})\Omega_{MS}+Y_{[2]11}\Omega_{MA}]$
	2^+_M	$\frac{3}{2}$	$\frac{1}{2}$	$\psi_{22}\frac{1}{\sqrt{2}}[\frac{1}{\sqrt{2}}(Y_{[2]20}-Y_{[2]02})\phi_{MS}+Y_{[2]11}\phi_{MA}]\chi_S$
	0^+_M	$\frac{3}{2}$	$\frac{1}{2}$	$\psi_{22}\frac{1}{\sqrt{2}}[Y_{[2]00}\phi_{MS}+Y_{[2]11}\phi_{MA}]\chi_S$
	2^+_S	$\frac{1}{2}$	$\frac{1}{2}$	$\psi_{22}\frac{1}{\sqrt{2}}[Y_{[2]20}+Y_{[2]02}]\Omega_S$
$F15$	2^+_M	$\frac{1}{2}$	$\frac{1}{2}$	$\psi_{22}\frac{1}{\sqrt{2}}[\frac{1}{\sqrt{2}}(Y_{[2]20}-Y_{[2]02})\Omega_{MS}+Y_{[2]11}\Omega_{MA}]$
	2^+_M	$\frac{3}{2}$	$\frac{1}{2}$	$\psi_{22}\frac{1}{\sqrt{2}}[\frac{1}{\sqrt{2}}(Y_{[2]20}-Y_{[2]02})\phi_{MS}+Y_{[2]11}\phi_{MA}]\chi_S$
	2^+_S	$\frac{1}{2}$	$\frac{1}{2}$	$\psi_{22}\frac{1}{\sqrt{2}}[Y_{[2]20}+Y_{[2]02}]\Omega_S$
$F17$	2^+_M	$\frac{3}{2}$	$\frac{1}{2}$	$\psi_{22}\frac{1}{\sqrt{2}}[\frac{1}{\sqrt{2}}(Y_{[2]20}-Y_{[2]02})\phi_{MS}+Y_{[2]11}\phi_{MA}]\chi_S$
$P31$	2^+_S	$\frac{3}{2}$	$\frac{3}{2}$	$\psi_{22}\frac{1}{\sqrt{2}}[(Y_{[2]20}+Y_{[2]02}]\chi_S\phi_S$
	0^+_M	$\frac{1}{2}$	$\frac{3}{2}$	$\psi_{22}\frac{1}{\sqrt{2}}[Y_{[2]00}\chi_{MS}+Y_{[2]11}\chi_{MA}]\phi_S$
$P33$	0^+_S	$\frac{3}{2}$	$\frac{3}{2}$	$\psi_{00}Y_{[0]00}\chi_S\phi_S$
	0^+_S	$\frac{3}{2}$	$\frac{3}{2}$	$\psi_{10}Y_{[0]00}\chi_S\phi_S$
	0^+_S	$\frac{3}{2}$	$\frac{3}{2}$	$\psi_{20}Y_{[0]00}\chi_S\phi_S$
	2^+_S	$\frac{3}{2}$	$\frac{3}{2}$	$\psi_{22}\frac{1}{\sqrt{2}}[Y_{[2]20}+Y_{[2]02}]\chi_S\phi_S$
	2^+_M	$\frac{1}{2}$	$\frac{3}{2}$	$\psi_{22}\frac{1}{\sqrt{2}}[\frac{1}{\sqrt{2}}(Y_{[2]20}-Y_{[2]02})\chi_{MS}+Y_{[2]11}\chi_{MA}]\phi_S$
$F35$	2^+_M	$\frac{1}{2}$	$\frac{3}{2}$	$\psi_{22}\frac{1}{\sqrt{2}}[\frac{1}{\sqrt{2}}(Y_{[2]20}-Y_{[2]02})\chi_{MS}+Y_{[2]11}\chi_{MA}]\phi_S$
	2^+_S	$\frac{3}{2}$	$\frac{3}{2}$	$\psi_{22}\frac{1}{\sqrt{2}}[Y_{[2]20}+Y_{[2]02}]\chi_S\phi_S$
$F37$	2^+_S	$\frac{3}{2}$	$\frac{3}{2}$	$\psi_{22}\frac{1}{\sqrt{2}}[Y_{[2]20}+Y_{[2]02}]\chi_S\phi_S$

terest in this article. In these Tables, the second, third and fourth columns show the angular momentum, $L^P_{S_3}$, the spin, S, and isospin, T. States are shown in the last column. They are written in terms of the hyperradial wave functions, $\psi_{\omega\gamma}$, of Table 2, of the hyperspherical harmonics, $(Y_{[\gamma]})_{S_3}$, of Table 1, of the spin states, χ_{MS}, χ_{MA}, χ_S, defined as

$$\chi_{MS} = |((\frac{1}{2},\frac{1}{2})1,\frac{1}{2})\frac{1}{2}>, \tag{1}$$

$$\chi_{MA} = |((\frac{1}{2},\frac{1}{2})0,\frac{1}{2})\frac{1}{2}>, \tag{2}$$

$$\chi_S = |((\frac{1}{2},\frac{1}{2})1,\frac{1}{2})\frac{3}{2}>, \tag{3}$$

and of the isospin states ϕ_{MS}, ϕ_{MA}, ϕ_S, defined in a similar way. In order to simplify the notation, the following combinations of spin and isospin wave functions with definite S_3 symmetry are used

$$\Omega_S = \frac{1}{\sqrt{2}}[\chi_{MA}\phi_{MA}+\chi_{MS}\phi_{MS}], \tag{4}$$

$$\Omega_{MS} = \frac{1}{\sqrt{2}}[\chi_{MA}\phi_{MA}-\chi_{MS}\phi_{MS}], \tag{5}$$

$$\Omega_{MA} = \frac{1}{\sqrt{2}}[\chi_{MA}\phi_{MS}+\chi_{MS}\phi_{MA}], \tag{6}$$

$$\Omega_A = \frac{1}{\sqrt{2}}[\chi_{MA}\phi_{MS}-\chi_{MS}\phi_{MA}], \tag{7}$$

Table 7. Three quark states with negative parity

Resonances	$L^P_{S_3}$	S	T	States
$S11$	1^-_M	$\frac{1}{2}$	$\frac{1}{2}$	$\psi_{11}\frac{1}{\sqrt{2}}[Y_{[1]10}\Omega_{MA}+Y_{[1]01}\Omega_{MS}]$
	1^-_M	$\frac{1}{2}$	$\frac{1}{2}$	$\psi_{21}\frac{1}{\sqrt{2}}[Y_{[1]10}\Omega_{MA}+Y_{[1]01}]\Omega_{MS}$
	1^-_M	$\frac{3}{2}$	$\frac{1}{2}$	$\psi_{11}\frac{1}{\sqrt{2}}[Y_{[1]10}\phi_{MA}+Y_{[1]01}\phi_{MS}]\chi_S$
	1^-_M	$\frac{3}{2}$	$\frac{1}{2}$	$\psi_{21}\frac{1}{\sqrt{2}}[Y_{[1]10}\phi_{MA}+Y_{[1]01}\phi_{MS}]\chi_S$
$D13$	1^-_M	$\frac{1}{2}$	$\frac{1}{2}$	$\psi_{11}\frac{1}{\sqrt{2}}[Y_{[1]10}\Omega_{MA}+Y_{[1]01}\Omega_{MS}]$
	1^-_M	$\frac{1}{2}$	$\frac{1}{2}$	$\psi_{21}\frac{1}{\sqrt{2}}[Y_{[1]10}\Omega_{MA}+Y_{[1]01}]\Omega_{MS}$
	1^-_M	$\frac{3}{2}$	$\frac{1}{2}$	$\psi_{11}\frac{1}{\sqrt{2}}[Y_{[1]10}\phi_{MA}+Y_{[1]01}\phi_{MS}]\chi_S$
	1^-_M	$\frac{3}{2}$	$\frac{1}{2}$	$\psi_{21}\frac{1}{\sqrt{2}}[Y_{[1]10}\phi_{MA}+Y_{[1]01}\phi_{MS}]\chi_S$
$D15$	1^-_M	$\frac{3}{2}$	$\frac{1}{2}$	$\psi_{11}\frac{1}{\sqrt{2}}[Y_{[1]10}\phi_{MA}+Y_{[1]01}\phi_{MS}]\chi_S$
	1^-_M	$\frac{3}{2}$	$\frac{1}{2}$	$\psi_{21}\frac{1}{\sqrt{2}}[Y_{[1]10}\phi_{MA}+Y_{[1]01}\phi_{MS}]\chi_S$
$S31$	1^-_M	$\frac{1}{2}$	$\frac{3}{2}$	$\psi_{11}\frac{1}{\sqrt{2}}[Y_{[1]10}\chi_{MA}+Y_{[1]01}\chi_{MS}]\phi_S$
	1^-_M	$\frac{1}{2}$	$\frac{3}{2}$	$\psi_{21}\frac{1}{\sqrt{2}}[Y_{[1]10}\chi_{MA}+Y_{[1]01}\chi_{MS}]\phi_S$
$S33$	1^-_M	$\frac{1}{2}$	$\frac{3}{2}$	$\psi_{11}\frac{1}{\sqrt{2}}[Y_{[1]10}\chi_{MA}+Y_{[1]01}\chi_{MS}]\phi_S$
	1^-_M	$\frac{1}{2}$	$\frac{3}{2}$	$\psi_{21}\frac{1}{\sqrt{2}}[Y_{[1]10}\chi_{MA}+Y_{[1]01}\chi_{MS}]\phi_S$

The coupling of the orbital, L, and spin, S, angular momentum to the total angular momentum J is not shown in these Tables. The color part, a SU(3) singlet, is also omitted for simplicity.

References

1. R. Bijker, F. Iachello and A. Leviatan, Ann. Phys. (N.Y.) **236**, 69 (1994)
2. S. Capstick and B.D. Keister, Phys. Rev. **D51**, 3598 (1995)
3. F. Cardarelli, E. Pace, G. Salmé and S. Simula, Phys. Lett. **B332**, 1 (1994); Phys. Rev. **D 53**, 6682 (1996); Phys. Lett. **B349**, 393 (1995);Phys. Lett. **B359**, 1 (1995)
4. M. Ferraris, M.M. Giannini, M. Pizzo, E. Santopinto and L. Tiator, Phys. Lett. **B364**, 231 (1995); M. Aiello, M. Ferraris, M.M. Giannini, M. Pizzo and E. Santopinto, Phys. Lett. **B387**, 215 (1996)
5. A. Valcarce, P. González, P. Fernández and V. Vento, Phys. Lett. **B367**, 35 (1996)
6. Z. Dziembowski, M. Fabre de la Ripelle and Gerald A. Miller, Phys. Rev. **C53**, R2038 (1996)
7. L. Ya. Glozman and D. O. Riska, Phys. Rep. **268**, (1996); L. Ya. Glozman, Z. Papp and W. Plessas, Phys. Lett. (in print)
8. M. Benmerrouche, N. C. Mukhopadhyay and J.-F. Zhang, Phys. Rev. Lett. **77**, 4716 (1996)
9. N. Isgur and G. Karl, Phys. Rev. **D18**, 4187 (1978); **D19**, 2653 (1979); **D20**, 1191 (1979)
10. S. Capstick and N. Isgur, Phys. Rev. **D 34**,2809 (1986)
11. M.M. Giannini, Rep. Prog. Phys. **54**, 453 (1991)
12. M. Warns, W. Pfeil and H. Rollnik, Phys. Rev. **D42**, 2215 (1990)
13. L. A. Copley, G. Karl and E. Obryk, Phys. Lett. **29**, 117 (1969)
14. R. Koniuk and N. Isgur, Phys. Rev. **D21**, 1868 (1980)
15. G. Morpurgo, Nuovo Cimento **9**, 461 (1952); Yu. A. Simonov, Sov. J. Nucl. Phys. **3**, 461 (1966)
16. J. Ballot and M. Fabre de la Ripelle, Ann. of Phys. (N.Y.) **127**, 62 (1980)
17. P. Hasenfratz, R.R. Horgan, J. Kuti and J.M. Richard, Phys. Lett. **B94**, 401 (1980)
18. L. Heller, in "Quarks and Nuclear Forces", eds. D.C. Vries and B. Zeitnitz, Springer Tracts in Modern Physics **100**, 145 (1982)
19. J. Carlson, J. Kogut and V.R. Pandharipande, Phys. Rev. **D27**, 233 (1983)
20. M.M. Giannini, Nuovo Cimento **A76**, 455 (1983); D. Drechsel, M.M. Giannini and L. Tiator, in "The Three-Body Force in the Three-Nucleon System", eds. B.L. Berman and B.F. Gibson, Lecture Notes in Physics **260**, 509 (1986); Few-Body Syst. Suppl. **2**, J.-L. Ballot and M. Fabre de la Ripelle eds., 448 (1987)
21. E. Santopinto, M.M. Giannini and F. Iachello, in "Symmetries in Science VII", ed. B. Gruber, Plenum Press, New York, 445 (1995); F. Iachello, in "Symmetries in Science VII", ed. B. Gruber, Plenum Press, New York, 213 (1995)
22. M. Fabre de la Ripelle and J. Navarro, Ann. Phys. (N.Y.) **123**, 185 (1979)
23. J.-M. Richard and P. Taxil, Ann. Phys. (N.Y.) **150**, 3267 (1983)
24. J.-L. Basdevant and P. Boukraa, Z. Phys. **C 30**, 103 (1986)
25. A. M. Badalyan,Phys. Lett. **B199**,267 (1987)
26. J. Leal Ferreira and P. Leal Ferreira, Lett. Nuovo Cimento vol. III, 43 (1970)
27. H.J. Lipkin, Rivista Nuovo Cimento I (volume speciale), 134 (1969)
28. A. M. Perelemov and V. S. Popov, Sov. J. Nucl. Phys. **6**, 819 (1966)
29. P. Morse and H. Feshbach, Methods of Theoretical Physics, Mc Graw-Hill, New York (1953)
30. Yu. A. Simonov, Sov. J. Nucl. Phys. **3**, 461 (1966); **7**, 722 (1968)
31. M.I. Haftel and V. B. Mandelzweig, Ann. Phys. (N.Y.) **150**, 48 (1983)
32. H. Høgaasen and J.-M. Richard, Phys. Lett. **B124**, 520 (1983)
33. M. Campostrini, K. Moriarty and C. Rebbi, Phys. Rev. **D36**, 3450 (1987)
34. R.M. Barnett et al. (Particle Data Group), Phys. Rev. **D54**, 1 (1996)
35. R. McClary and N. Byers, Phys. Rev. **D28**, 1692 (1983); F. Iachello and D. Kusnezov, Phys. Rev. **D45**, 4156 (1992)
36. V. Burkert, private communication